Supporting Information

Tunable upconversion of holmium sublattice through interfacial energy transfer for anti-counterfeiting

Rong Huang,[a] Songbin Liu,[a] Jinshu Huang,[a] Huiming Liu,[a] Zhiyong Hu,[a] Lili Tao[b] and Bo Zhou[a]**

[a] State Key Laboratory of Luminescent Materials and Devices, Guangdong Provincial Key Laboratory of Fiber Laser Materials and Applied Techniques, Guangdong Engineering Technology Research and Development Center of Special Optical Fiber Materials and Devices, South China University of Technology, Guangzhou 510641, China.

E-mail: zhoubo@scut.edu.cn

[b] School of Materials and Energy, Guangdong University of Technology, Guangzhou 510006, China.

E-mail: taoll@gdut.edu.cn

Supporting Tables S1~S5

Table S1. CIE coordinates of the visible emission profiles from the samples in Fig. 2d under 980 nm excitation.

$NaHoF_4$:Yb(x mol%)@$NaYF_4$	CIE *x*	CIE *y*
x = 5	0.682	0.302
x = 10	0.693	0.300
x = 20	0.686	0.310
x = 30	0.640	0.354
x = 40	0.565	0.427
x = 50	0.412	0.575
x = 60	0.347	0.637

Table S2. CIE coordinates of the visible emission profiles from the samples in Fig. 4a under 980 nm excitation.

$NaHoF_4$@$NaYF_4$:Yb(x mol%)	CIE *x*	CIE *y*
x = 5	0.669	0.311
x = 10	0.654	0.329
x = 20	0.694	0.298
x = 40	0.671	0.318
x = 60	0.639	0.343
x = 80	0.595	0.385
x = 100	0.497	0.480

Table S3. CIE coordinates of the visible emission profiles from the samples in Fig. 6b under 808 nm excitation.

$NaHoF_4$@$NaYF_4$:Yb(x mol%)@$NaYF_4$:Nd/Yb(30/20 mol%)	CIE *x*	CIE *y*
x = 20	0.677	0.315
x = 40	0.653	0.330
x = 60	0.597	0.389
x = 80	0.566	0.417
x = 100	0.473	0.507

Table S4. CIE coordinates of the visible emission profiles from the samples in Fig. S8a under 980 nm excitation.

$NaHoF_4$@$NaYF_4$:Yb(x mol%)@$NaYF_4$:Nd/Yb(30/20 mol%)	CIE *x*	CIE *y*
x = 20	0.688	0.306
x = 40	0.662	0.326
x = 60	0.610	0.377
x = 80	0.572	0.412
x = 100	0.475	0.506

Table S5. CIE coordinates of the visible emission profiles from the $NaYF_4$:Ho(40 mol%)@$NaYF_4$:Yb(60 mol%)@$NaYF_4$ core-shell-shell nanoparticles under 980 nm excitation.

980 nm Excitation	CIE *x*	CIE *y*
CW	0.619	0.378
2 ms	0.533	0.461
1 ms	0.488	0.504
500 μs	0.449	0.543
300 μs	0.432	0.559

Supporting Figures S1~S17

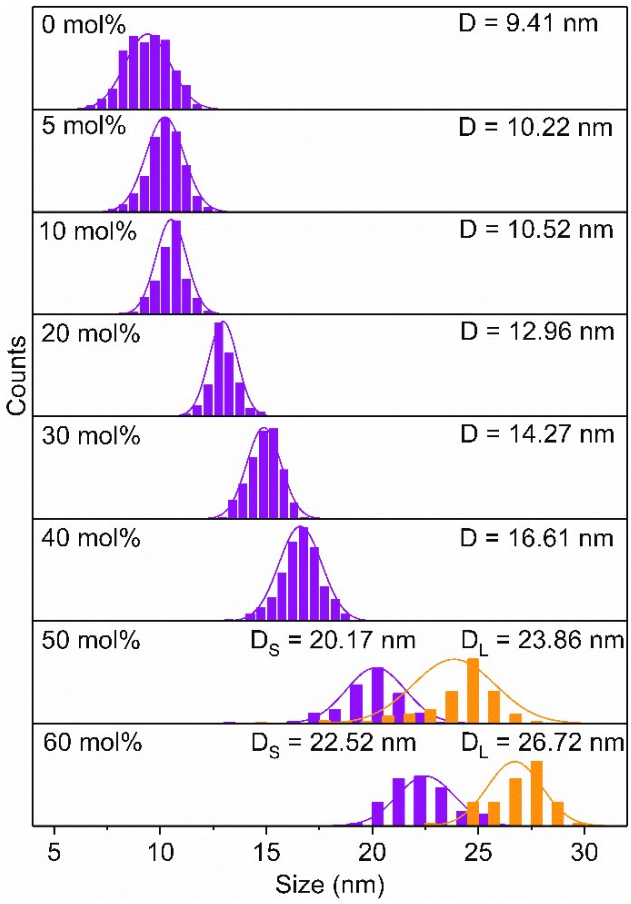

Figure S1. Size distribution of as-synthesized $NaHoF_4:Yb^{3+}$(0~60 mol%) nanoparticles indicating an increase of the average size with increasing Yb^{3+} concentration. Note that the D_S and D_L stand for short diameter and long diameter, respectively.

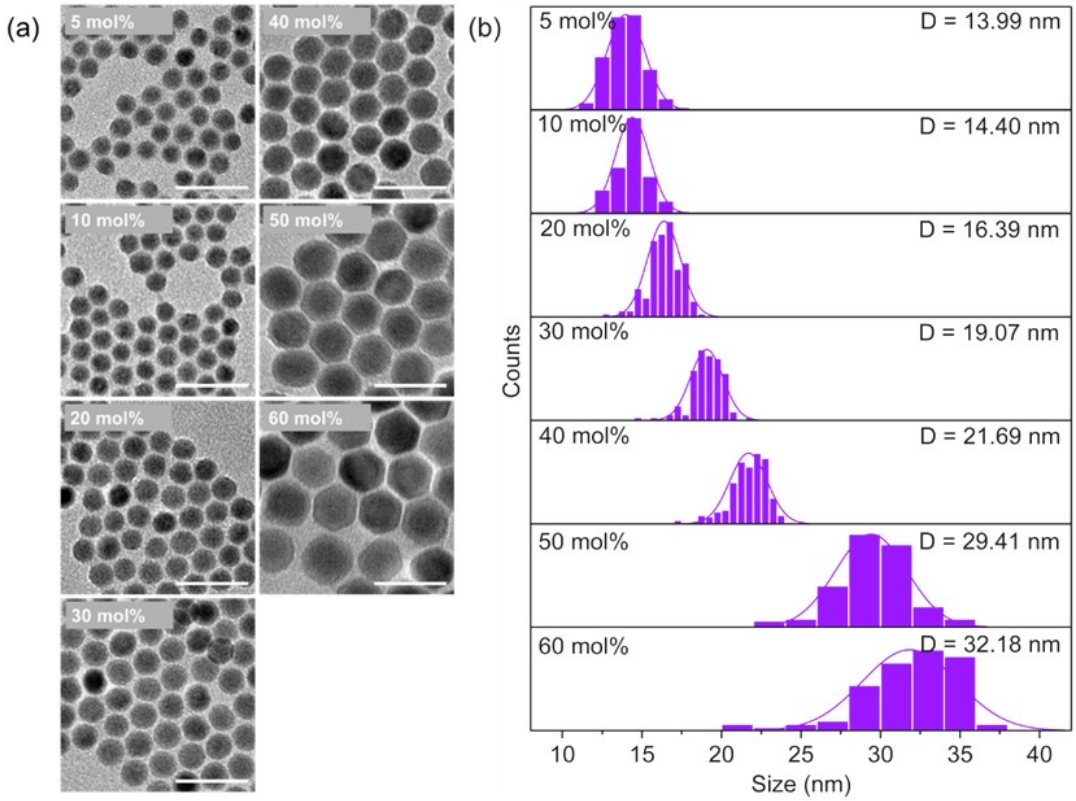

Figure S2. (a) TEM images and (b) corresponding size-distributions of as-synthesized $NaHoF_4$:Yb^{3+}(0~60 mol%)@$NaYF_4$ nanoparticles showing an obvious increase in particle size. Scale bars, 50 nm.

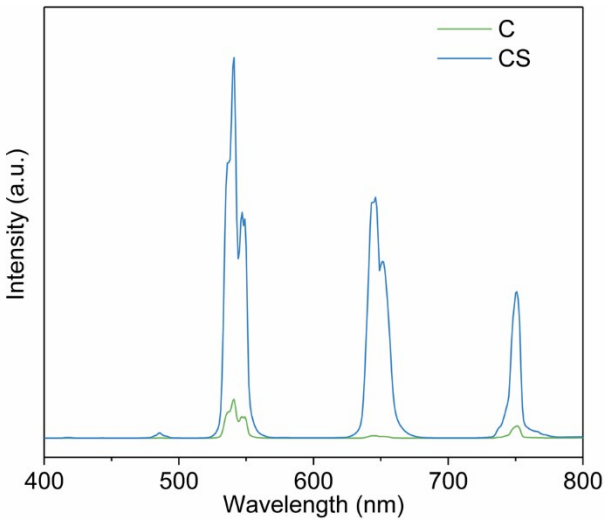

Figure S3. Upconversion emission spectra of $NaHoF_4$:Yb(60 mol%) core (C) and $NaHoF_4$:Yb(60 mol%)@$NaYF_4$ core-shell (CS) nanoparticles under 980 nm excitation.

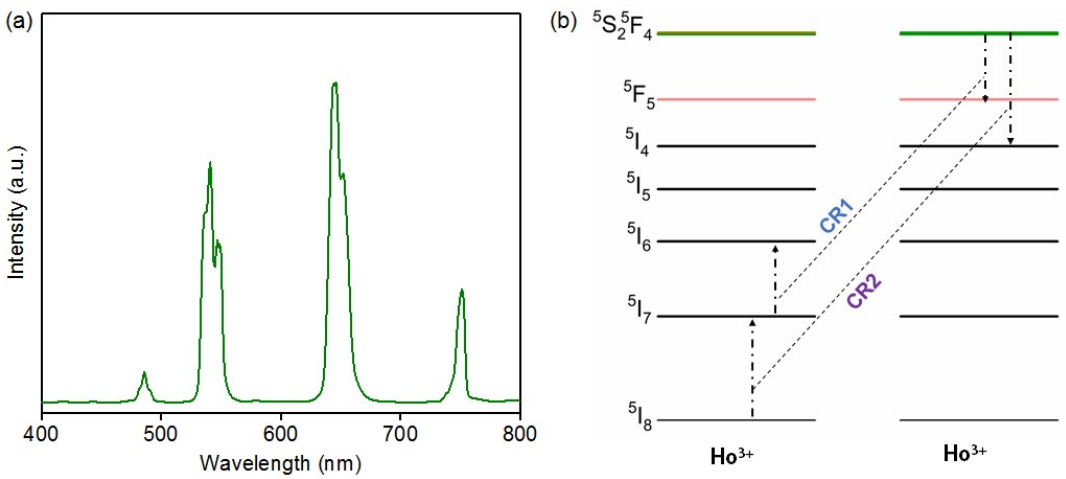

Figure S4. (a) Upconversion emission spectrum of $NaYF_4$:Yb/Ho(20/2 mol%)@$NaYF_4$ nanoparticles under 980 nm excitation. (b) Schematic of possible cross relaxation processes in heavy Ho^{3+} concentration that may quench the green emitting level. CR1: [($^5S_2$, $^5F_4$); $^5I_7$] → [$^5F_5$; $^5I_6$], CR2: [($^5S_2$, $^5F_4$); $^5I_8$] → [$^5I_4$; $^5I_7$].

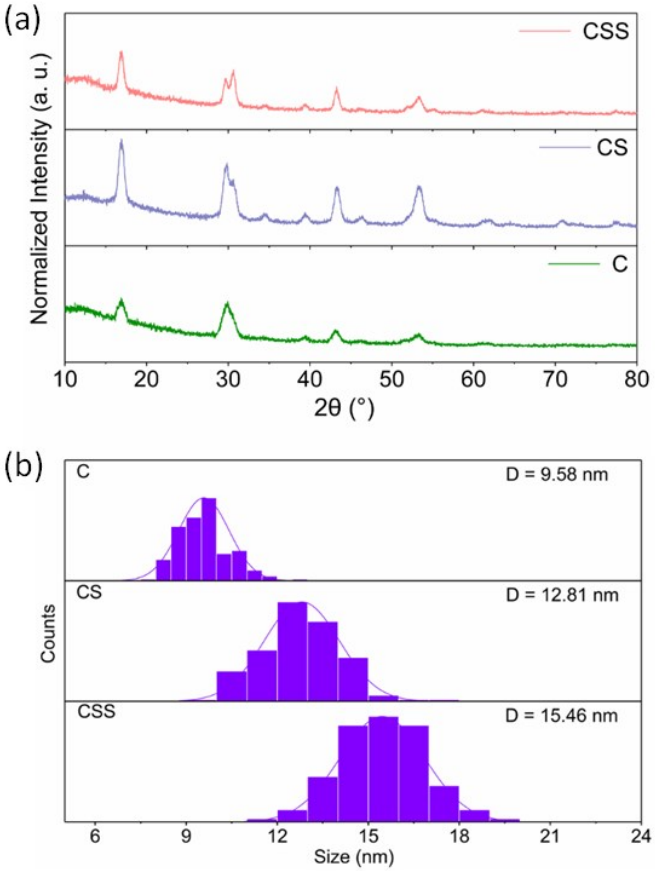

Figure S5. (a) X-ray diffraction patterns of as-prepared $NaYF_4$:Ho(40 mol%) core (C), $NaYF_4$:Ho(40 mol%)@$NaYF_4$:Yb(60 mol%) core-shell (CS) and $NaYF_4$:Ho(40 mol%)@$NaYF_4$:Yb(60 mol%)@$NaYF_4$ core-shell-shell (CSS) nanoparticles. (b) Size distributions of the (a) samples. Note that their TEM images were shown in Fig. 3a in the main text.

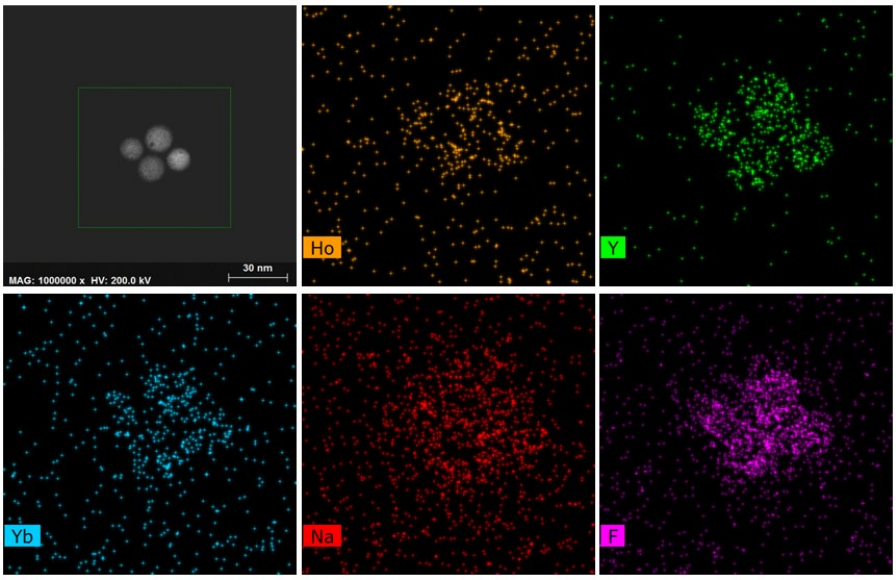

Figure S6. STEM image and element mappings of Ho, Y, Yb, Na and F for the $NaYF_4$:Ho(40 mol%)@$NaYF_4$:Yb(60 mol%)@$NaYF_4$ core-shell-shell nanoparticles.

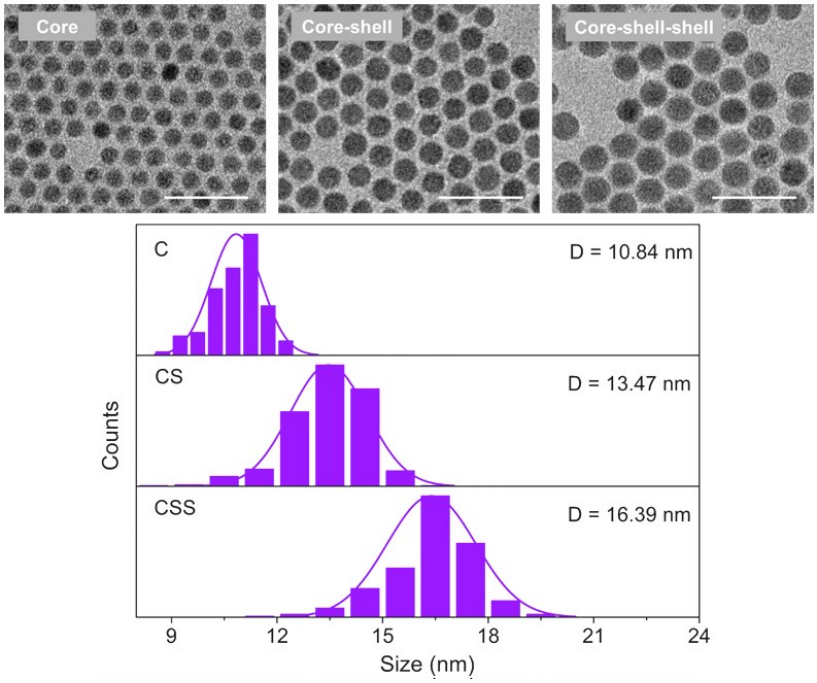

Figure S7. TEM images (top) and their size distributions (bottom) of the $NaYF_4$:Ho(20 mol%) core (C), $NaYF_4$:Ho(20 mol%)@$NaYF_4$:Yb(60 mol%) core-shell (CS), and $NaYF_4$:Ho(20 mol%)@$NaYF_4$:Yb(60 mol%)@$NaYF_4$ core-shell-shell (CSS) nanoparticles. Scale bars of the TEM images are 50 nm.

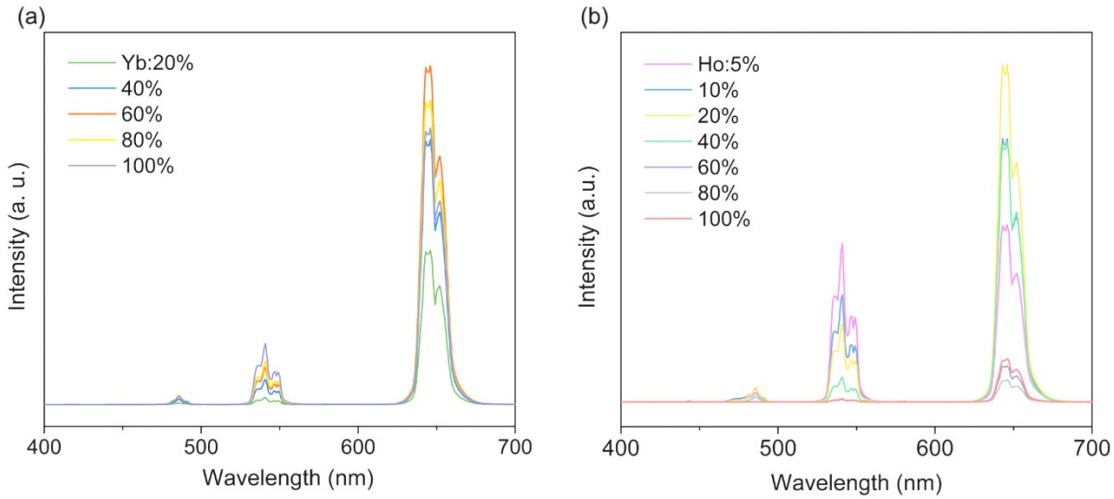

Figure S8. Upconversion emission spectra of (a) $NaYF_4$:Ho(40 mol%)@$NaYF_4$:Yb(20~100 mol%)@$NaYF_4$ and (b) $NaYF_4$:Ho(5~100 mol%)@$NaYF_4$:Yb(60 mol%)@$NaYF_4$ core-shell-shell nanoparticles. Note that the concentration of Ho^{3+} at 20 mol% in the core and Yb^{3+} at 60 mol% in the interlayer present the best upconversion emission.

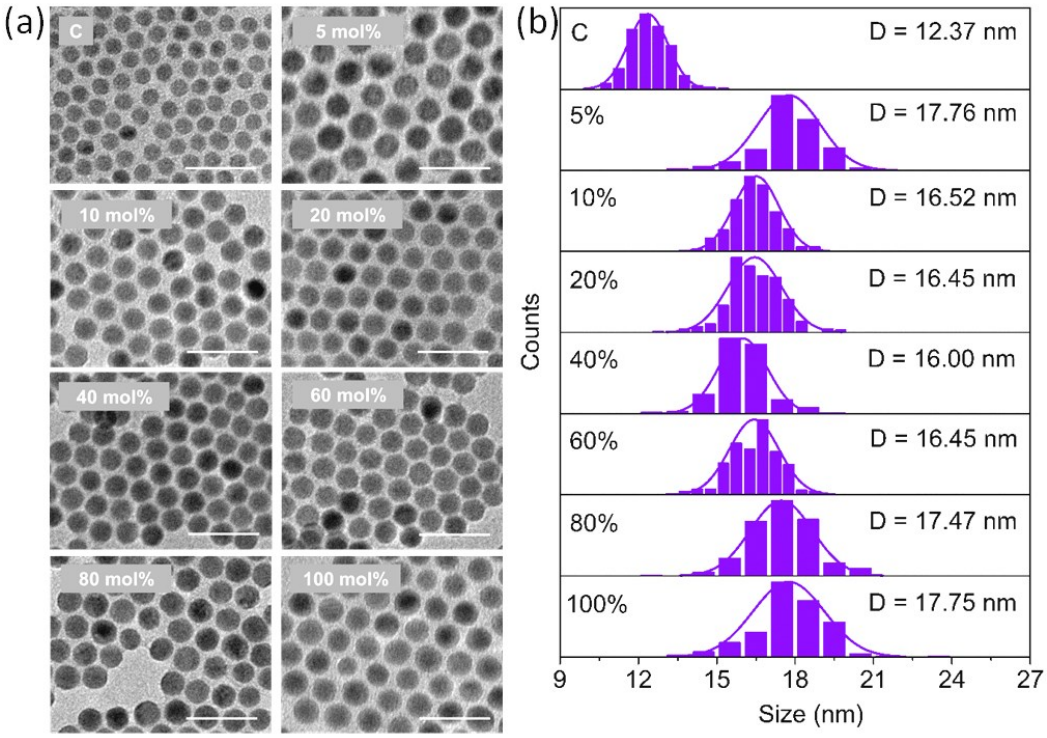

Figure S9. (a) TEM images and (b) their size distributions of the $NaHoF_4$ core (C) and $NaHoF_4$@$NaYF_4$:Yb(5~100 mol%) core-shell nanoparticles. Scale bars of the TEM images are 50 nm.

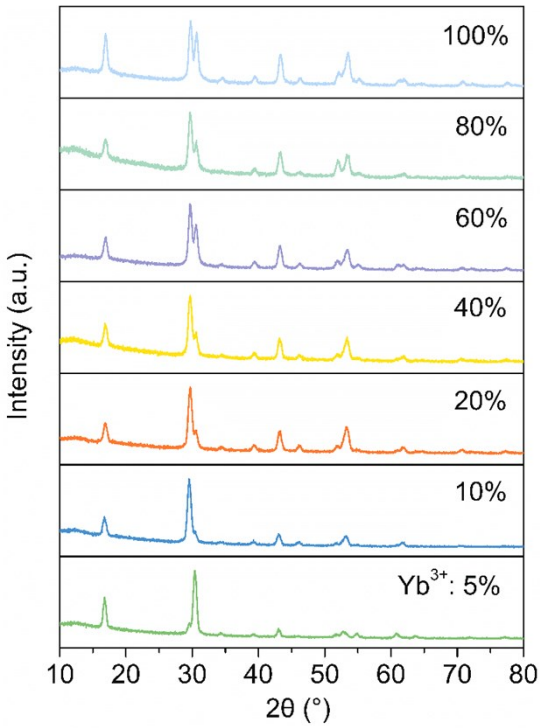

Figure S10. X-ray diffraction patterns of the $NaHoF_4$@$NaYF_4$:Yb(5~100 mol%) core-shell nanoparticles.

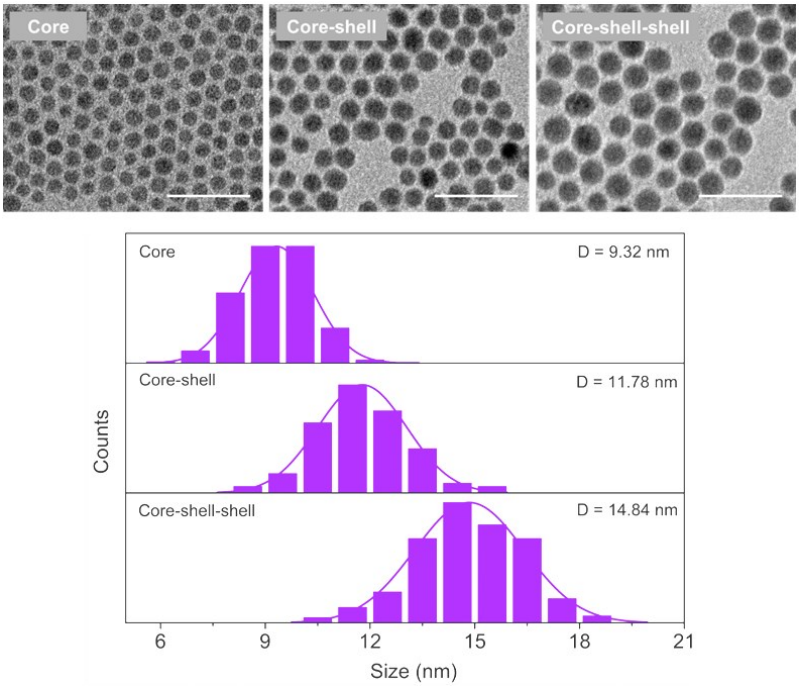

Figure S11. TEM images (top) and their size distributions (bottom) of the $NaHoF_4$ core, $NaHoF_4$@$NaYF_4$:Yb(20 mol%) core-shell, and $NaHoF_4$@$NaYF_4$:Yb(20 mol%)@$NaYF_4$ core-shell-shell nanoparticles. Scale bars of the TEM images are 50 nm.

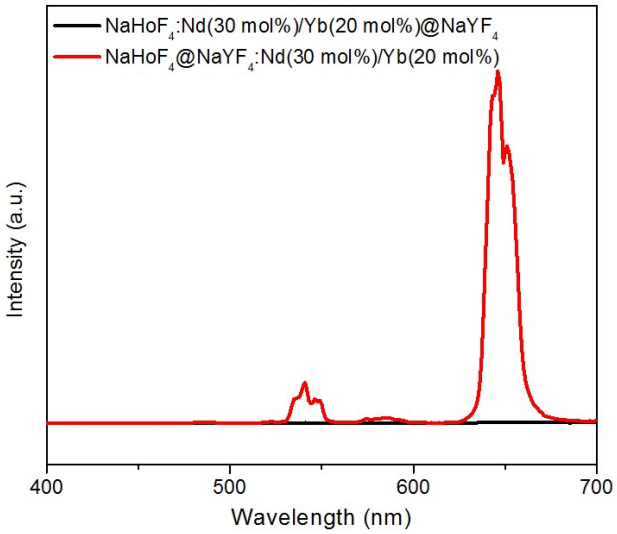

Figure S12. A comparison of the upconversion emission spectra from the $NaHoF_4$@$NaYF_4$:Nd/Yb(30/20 mol%) and $NaHoF_4$:Nd/Yb(30/20 mol%)@$NaYF_4$ core-shell nanoparticles under 808 nm excitation.

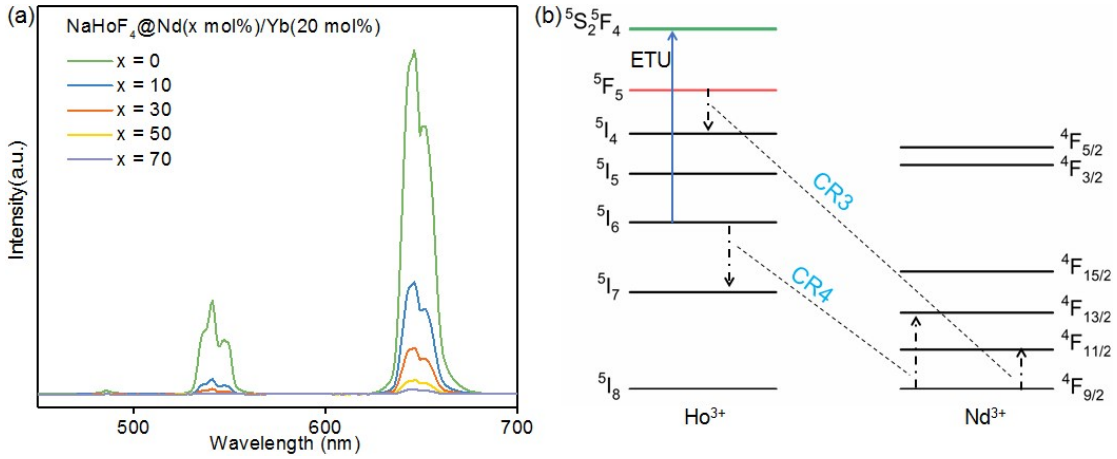

Figure S13. (a) Upconversion emission spectra of $NaHoF_4$@$NaHoF_4$:Nd/Yb(0~70/20 mol%) core-shell nanoparticles under 980 nm excitation. (b) Schematic of possible cross relaxation processes between Ho^{3+} and Nd^{3+} that may quench the Ho^{3+} emissions under 980 nm excitation. CR3: [Ho^{3+}($^5F_5$); Nd^{3+}($^4F_{9/2}$)] → [Ho^{3+}($^5I_4$); Nd^{3+}($^4F_{11/2}$)], CR4: [Ho^{3+}($^5I_6$); Nd^{3+}($^4F_{9/2}$)] → [Ho^{3+}($^5I_7$); Nd^{3+}($^4F_{13/2}$)].

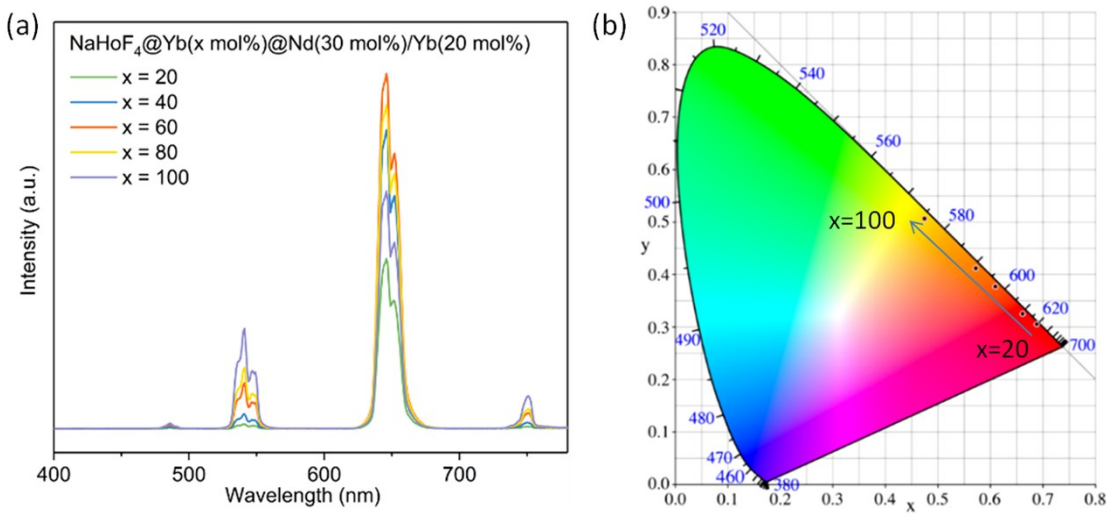

Figure S14. (a) Upconversion emission spectra of $NaHoF_4$@$NaYF_4$:Yb(20~100 mol%)@$NaYF_4$:Nd/Yb(30/20 mol%) core-shell-shell nanoparticles under 980 nm excitation. (b) CIE coordinates of the emission profiles in (a).

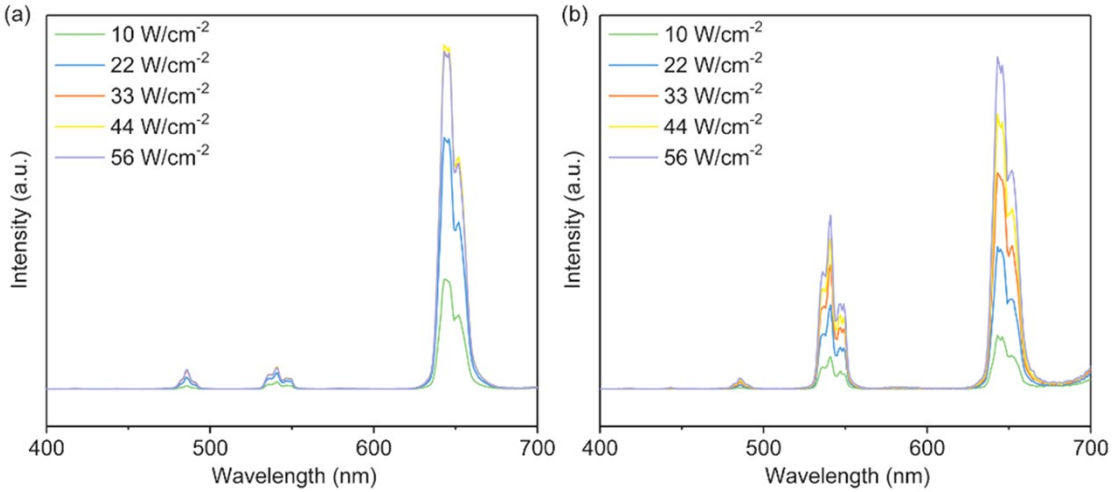

Figure S15. Dependence of the upconversion emission intensity for the (a) $NaHoF_4$@$NaYF_4$:Yb(40 mol%)@$NaYF_4$:Nd/Yb(30/20 mol%) and (b) $NaHoF_4$@$NaYbF_4$@$NaYF_4$:Nd/Yb(30/20 mol%) samples under 808 nm excitation with different power densities.

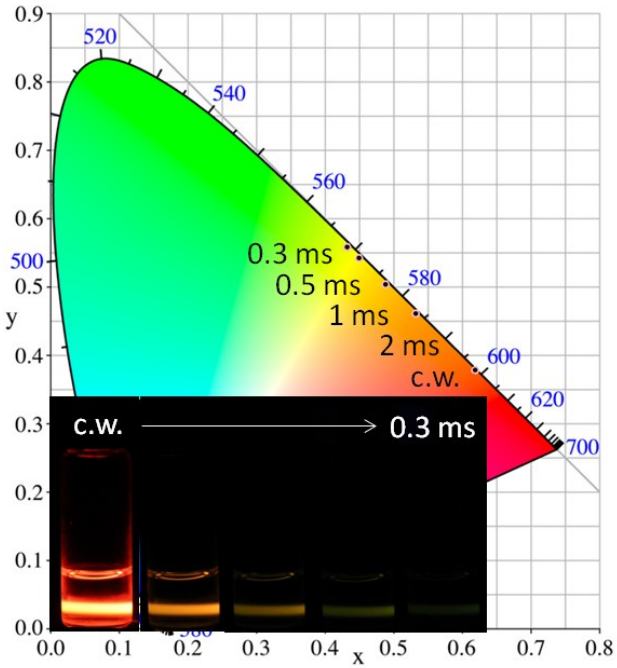

Figure S16. CIE coordinates of the emission in the $NaYF_4$:Ho(40 mol%)@$NaYF_4$:Yb(60 mol%)@$NaYF_4$ core-shell-shell nanoparticles under pulsed 980 nm excitation with different pulse widths. Inset shows the corresponding emission photographs.

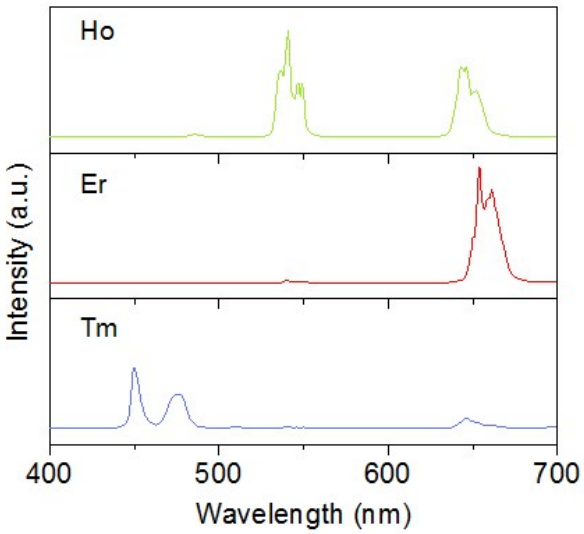

Figure S17. Upconversion emission spectra of the $NaYF_4$:Yb/Tm(30/1 mol%)@$NaYF_4$, $NaErF_4$@$NaYF_4$, and $NaYF_4$:Yb/Ho(20/2 mol%)@$NaYF_4$ core-shell nanoparticles under 980 nm excitation.